



Design of boundary combined footings of rectangular shape using a new model

Arnulfo Luévanos-Rojas

University of Durango State, Gómez Palacio, Durango, México. arnulfol_2007@hotmail.com

Received: January 28th, 2014. Received in revised form: August 6th, 2014. Accepted: August 11th, 2014.

Abstract

This paper presents the design of boundary combined footings of rectangular shape using a new model to consider real soil pressure acting on the contact surface of the footing; such pressure is presented in terms of an axial load, moment around the "X" axis and moment around the "Y" axis to each column. The classic model considers an axial load and moment around the transverse axis applied in each column, and when the moments in two directions are taken into account, the maximum pressure throughout the contact surface of the footing is considered the same. The main part of this research is that the proposed model considers real soil pressure and the classic model takes into account the maximum pressure and uniform is considered. It is concluded that the proposed model is more suited to the real conditions and is more economical.

Keywords: boundary combined footings; resultant force; center of gravity; bending moment; bending shear; punching shear.

Diseño de zapatas combinadas de lindero de forma rectangular utilizando un nuevo modelo

Resumen

Este documento presenta el diseño de zapatas combinadas de lindero de forma rectangular utilizando un nuevo modelo para considerar la presión real del suelo que actúan en la superficie de contacto de la zapata, dicha presión se presenta en función de una carga axial, momento alrededor del eje "X" y momento alrededor del eje "Y" de cada columna. El modelo clásico considera una carga axial y un momento alrededor del eje transversal aplicada en cada columna, y cuando los momentos en dos direcciones son tomados en cuenta, la presión máxima en toda la superficie de contacto de la zapata se considera la misma. La parte principal de esta investigación es que el modelo propuesto considera la presión real del suelo y el modelo clásico toma en cuenta la presión máxima y la considera uniforme. Se concluye que el nuevo modelo es el más apropiado, ya que se apega más a las condiciones reales y es más económico.

Palabras clave: zapatas combinadas de lindero; Fuerza resultante; Centro de gravedad; Momento flexionante; Fuerza cortante por flexión; Fuerza cortante por penetración.

1. Introduction

The foundation is the part of the structure which transmits the loads to the soil. Each building demands the need to solve a problem of foundation. The foundations are classified into superficial and deep, which have important differences: in terms of geometry, the behavior of the soil, its structural functionality and its constructive systems [1,2].

Superficial foundations may be of various types according to their function; isolated footing, combined footing, strip footing, or mat foundation [1-4].

The distribution of soil pressure under a footing is a function of the type of soil, the relative rigidity of the soil

and the footing, and the depth of foundation at level of contact between footing and soil. A concrete footing on sand will have a pressure distribution similar to Fig. 1(a). When a rigid footing is resting on sandy soil, the sand near the edges of the footing tends to displace laterally when the footing is loaded. This tends to decrease in soil pressure near the edges, whereas soil away from the edges of footing is relatively confined. On the other hand, the pressure distribution under a footing on clay is similar to Fig. 1(b). As the footing is loaded, the soil under the footing deflects in a bowl-shaped depression, relieving the pressure under the middle of the footing. For design purposes, it is common to assume the soil pressures are linearly distributed.



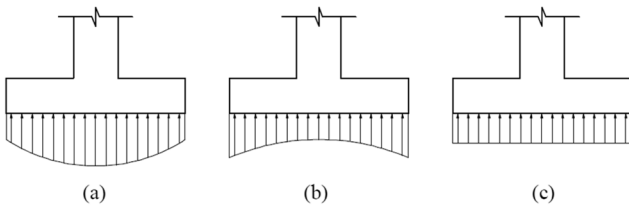


Figure 1. Pressure distribution under footing: (a) footing on sand; (b) footing on clay; (c) equivalent uniform distribution.

Source: Bowles, 1996

The pressure distribution will be uniform if the centroid of the footing coincides with the resultant of the applied loads, as shown in Fig. 1(c) [1].

In the design of superficial foundations, in the specific case of isolated footings, there are of three types in terms of the application of loads: 1) The footings subjected to concentric axial load, 2) The footings subjected to axial load and moment in one direction (unidirectional bending), 3) The footings subjected to axial load and moment in two directions (bidirectional bending) [1,2,5,6].

The hypothesis used in the classical model considers the axial load and moment around an axis transverse to the combined footing for the geometric proportions and shape are so fixed that the centroid of the footing area coincides with the resultant of the column loads. This results in uniform pressure below all the contact area of the footing. Then the equation of the bidirectional bending is used to obtain the stresses acting on the contact surface of the combined footings, which must meet the following conditions: 1) The minimum stress should be equal to or greater than zero, because the soil is not capable of withstand tensile stresses, 2) The maximum stress must be equal or less than the allowable capacity that can withstand the soil [1,2,5,6].

A combined footing is a long footing supporting two or more columns in (typically two) one row. The combined footing may be rectangular, trapezoidal or Tee-shaped in plan. Rectangular footing is provided when one of the projections of the footing is restricted or the width of the footing is restricted. Trapezoidal footing is provided when one column load is much more than the other. As a result, both projections of the footing beyond the faces of the columns will be restricted [7-9].

Some papers present the use of load testing on foundations: Non-destructive load test in pilots [10]; Evaluation of the integrity of deep foundations: analysis and in situ verification [11]; Other, shows the use of static load tests in the geotechnical design of foundations [12]; Comparison between resonant-column and bender element test on three types of soils [13].

Mathematical models have been developed to obtain the dimensions of rectangular, square and circular isolated footings subjected to axial load and moments in two directions (bidirectional bending) [14-16]. Also, a mathematical model was presented for design of isolated footings of rectangular shape using a new model [17].

This paper presents a full mathematical model for the design of boundary combined footings to obtain: 1) Moments around of an axis $a_1'-a_1'$ with a width " b_1' " and

$a_2'-a_2'$ with a width " b_2' " that are parallel to axis "Y-Y", and moments around of an axis $b'-b'$, $c'-c'$, $d'-d'$ and $e'-e'$ that are parallel to axis "X-X"; 2) Bending shear; 3) Punching shear for footings which support a boundary column and other inner column subject to axial load and moment in two directions (bidirectional bending), where pressures are different in the four corners, these pressures are presented in terms of the mechanical elements (axial load, moment around the axis "X-X" and moment around the axis "Y-Y").

2. Methodology

2.2. General conditions

According to Building Code Requirements for Structural Concrete (ACI 318-13) and Commentary the critical sections are: 1) the maximum moment is located in face of column, pedestal, or wall, for footings supporting a concrete column, pedestal, or wall; 2) bending shear is presented at a distance " d " (distance from extreme compression fiber to centroid of longitudinal tension reinforcement) shall be measured from face of column, pedestal, or wall, for footings supporting a column, pedestal, or wall; 3) punching shear is localized so that its perimeter " b_o " is a minimum but need not approach closer than " $d/2$ " to: (a) Edges or corners of columns, concentrated loads, or reaction areas; and (b) Changes in slab thickness such as edges of capitals, drop panels, or shear caps [18].

The general equation for any type of footings subjected to bidirectional bending [14-17, 19-21]:

$$\sigma = \frac{P}{A} \pm \frac{M_x C_y}{I_x} \pm \frac{M_y C_x}{I_y} \quad (1)$$

where: σ is the stress exerted by the soil on the footing (soil pressure), A is the contact area of the footing, P is the axial load applied at the center of gravity of the footing, M_x is the moment around the axis "X", M_y is the moment around the axis "Y", C_x is the distance in the direction "X" measured from the axis "Y" up to the farthest end, C_y is the distance in direction "Y" measured from the axis "X" up to the farthest end, I_y is the moment of inertia around the axis "Y" and I_x is the moment of inertia around the axis "X".

2.2. New model

Fig. 2 shows a combined footing supporting two rectangular columns of different dimensions (a boundary column and other inner column) subject to axial load and moments in two directions in each column.

Fig. 3 presents a combined footing due to the equivalent loads. The mechanical elements of the components P_1 , M_{x1} , M_{y1} are equivalent to a normal force " P_1 " acting on the point with coordinates (e_{x1}, e_{y1}) , and for the components of P_2 , M_{x2} , M_{y2} are equivalent to a normal force " P_2 " acting on the point with coordinates (e_{x2}, e_{y2}) .

The general equation of the bidirectional bending is:

$$\sigma = \frac{R}{ab} \pm \frac{6Ry_c}{ba^2} \pm \frac{6Rx_c}{ab^2} \leq \sigma_{adm} \quad (2)$$

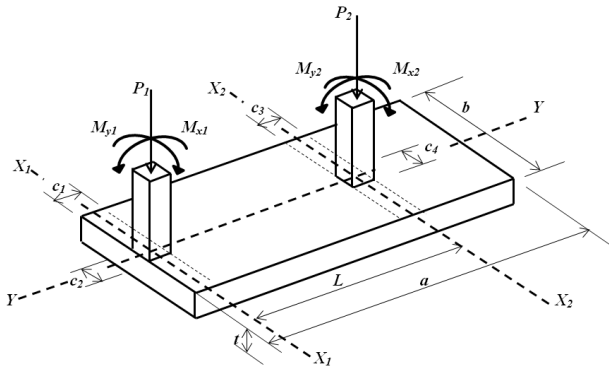


Figure 2. Boundary combined footing subjected to the real loads.
Source: Prepared by the author.

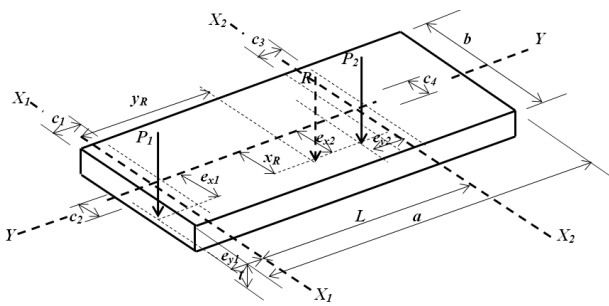


Figure 3. Combined footing due to the equivalent loads.
Source: Prepared by the author.

where: σ_{adm} is the capacity of available allowable load of the soil, R is the resultant force of the forces, y_c is the distance from the center of the contact area of the footing in the direction "Y" to the resultant, x_c is the distance from the center of the contact area of the footing in the direction "X" to the resultant.

Now the sum of moments around the axis "X_I" is obtained to find "y_R" and the resultant force is made to coincide with the gravity center of the area of the footing with the position of the resultant force in the direction "Y", therefore there is not moment around the axis "X" and the value of "y_c" is zero, " $x_R = x_c$ " is the sum of moments around the axis "Y" divided by the resultant, which is:

$$x_R = \frac{M_{y1} + M_{y2}}{P_1 + P_2} \quad (3)$$

Substituting equation (3) into equation (2) is transformed into a unidirectional bending system as follows:

$$\sigma = \frac{P_1 + P_2}{ab} \pm \frac{6(M_{y1} + M_{y2})}{ab^2} \leq \sigma_{adm} \quad (4)$$

Fig. 4 shows pressure diagram for combined footings subject to axial load and moment in one direction (unidirectional bending) in each column, where the pressures are presented at two different corners varying linearly along the contact surface, because there is not moment around the axis "X".

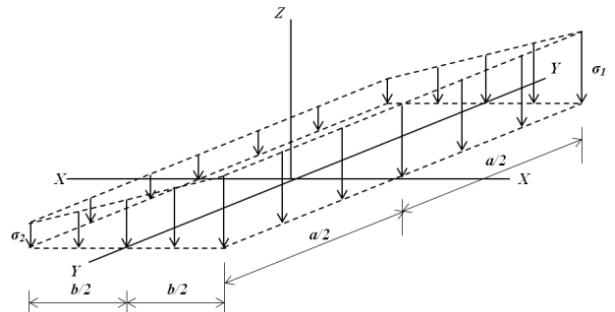


Figure 4. Pressure of the foundation on soil.
Source: Prepared by the author.

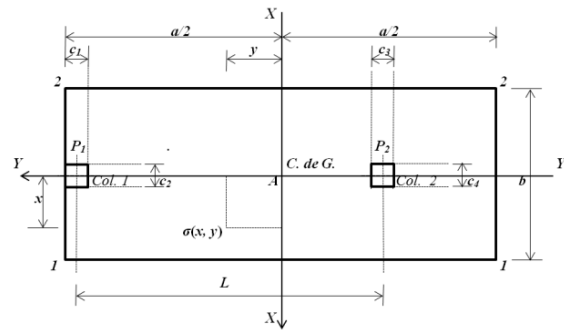


Figure 5. Boundary combined footing in plan.
Source: Prepared by the author.

Fig. 5 presents a boundary combined footing to obtain the stresses anywhere of the contact surface of the structural member due to the pressure that is exerted by the soil.

- In the longitudinal direction:

$$\sigma(x, y) = \frac{P_1 + P_2}{ab} + \frac{12(M_{y1} + M_{y2})x}{ab^3} \quad (5)$$

- In the transverse direction:

❖ To the boundary column is:

$$\sigma_{P_1}(x, y) = \frac{P_1}{b_1 b} + \frac{12M_{y1}x}{b_1 b^3} \quad (6)$$

❖ To the intermediate column is:

$$\sigma_{P_2}(x, y) = \frac{P_2}{b_2 b} + \frac{12M_{y2}x}{b_2 b^3} \quad (7)$$

where: $b_1 = c_1 + d/2$ is the width of the failure surface, $b_2 = c_3 + d$.

2.2.1. Model to obtain the bending moments

Critical sections for bending moments are shown in Fig. 6, these are presented in sections a'_1-a_1' , a'_2-a_2' , $b'-b'$, $c'-c'$, $d'-d'$ and $e'-e'$.

2.2.1.1. Moment around the axis a'_1-a_1'

The resultant force " F_{Ral} " is found through the volume

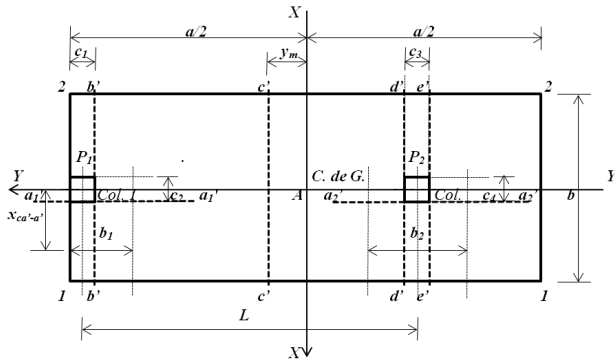


Figure 6. Critical sections for bending moments.

Source: Prepared by the author.

of pressure the area formed by the axis a_1' - a_1' with a width “ $b_1 = c_1 + d/2$ ” and the free end of the rectangular footing, where the higher pressure is presented:

$$F_{Ra_1'} = \int_{a/2-b_1}^{a/2} \int_{c_2/2}^{b/2} \sigma_{P_1}(x, y) dx dy = \frac{P_1(b - c_2)}{2b} + \frac{3M_{y1}(b^2 - c_2^2)}{2b^3} \quad (8)$$

The center of gravity “ $x_{ca_1'}$ ” is obtained by the equation:

$$x_{ca_1'} = \frac{\int_{a/2-b_1}^{a/2} \int_{c_2/2}^{b/2} x \sigma_{P_1}(x, y) dx dy}{\int_{a/2-b_1}^{a/2} \int_{c_2/2}^{b/2} \sigma_{P_1}(x, y) dx dy} = \frac{P_1 b^2 (b^2 - c_2^2) + 4M_{y1} (b^3 - c_2^3)}{4P_1 b^2 (b - c_2) + 12M_{y1} (b^2 - c_2^2)} \quad (9)$$

The moment around the axis a_1' - a_1' is:

$$M_{a_1'} = F_{Ra_1'}(x_{ca_1'} - c_2/2) \quad (10)$$

Substituting the equation (8) and (9) into equation (10) is obtained:

$$M_{a_1'} = \frac{(b - c_2)^2 [P_1 b^2 + 2M_{y1} (2b + c_2)]}{8b^3} \quad (11)$$

2.2.1.2. Moment around the axis a_2' - a_2'

The resultant force “ $F_{Ra_2'}$ ” is obtained through the volume of pressure the area formed by the axis a_2' - a_2' with a width “ $b_2 = c_3 + d$ ” and the free end of the rectangular footing, where the higher pressure is presented:

$$F_{Ra_2'} = \int_{(a-c_1-b_2)/2-L}^{(a-c_1+b_2)/2-L} \int_{c_4/2}^{b/2} \sigma_{P_2}(x, y) dx dy = \frac{P_2(b - c_4)}{2b} + \frac{3M_{y2}(b^2 - c_4^2)}{2b^3} \quad (12)$$

The center of gravity “ $x_{ca_2'}$ ” is obtained by the equation:

$$x_{ca_2'} = \frac{\int_{(a-c_1-b_2)/2-L}^{(a-c_1+b_2)/2-L} \int_{c_4/2}^{b/2} x \sigma_{P_2}(x, y) dx dy}{\int_{(a-c_1-b_2)/2-L}^{(a-c_1+b_2)/2-L} \int_{c_4/2}^{b/2} \sigma_{P_2}(x, y) dx dy} = \frac{P_2 b^2 (b^2 - c_4^2) + 4M_{y2} (b^3 - c_4^3)}{4P_2 b^2 (b - c_4) + 12M_{y2} (b^2 - c_4^2)} \quad (13)$$

The moment around the axis a_2' - a_2' is:

$$M_{a_2'} = F_{Ra_2'}(x_{ca_2'} - c_4/2) \quad (14)$$

Substituting the equation (12) and (13) into equation (14) is obtained:

$$M_{a_2'} = \frac{(b - c_4)^2 [P_2 b^2 + 2M_{y2} (2b + c_4)]}{8b^3} \quad (15)$$

2.2.1.3. Moment around the axis b' - b'

The resultant force “ $F_{Rb'}$ ” is the force “ P_1 ” acting on column 1 less the volume of pressure the area formed by the axis b' - b' and the corners 1 and 2 to the left of the footing, this is presented of the follows:

$$F_{Rb'} = P_1 - \int_{a/2-c_1}^{a/2} \int_{-b/2}^{b/2} \sigma(x, y) dx dy = P_1 - \frac{(P_1 + P_2)c_1}{a} \quad (16)$$

The center of gravity “ $y_{cb'}$ ” with respect to axis b' - b' is:

$$y_{cb'} = \frac{c_1}{2} \quad (17)$$

The moment around the axis b' - b' is:

$$M_{b'} = F_{Rb'}(y_{cb'}) \quad (18)$$

Substituting the equation (16) and (17) into equation (18) is obtained:

$$M_{b'} = \left[P_1 - \frac{(P_1 + P_2)c_1}{a} \right] \frac{c_1}{2} \quad (19)$$

2.2.1.4. Moment around the axis c' - c'

First, the position of the axis c' - c' must be localized, which is where the maximum moment is located.

When the shear force is zero, the moment should be the maximum, then the shear force is presented at a distance “ y_m ”, this is shown as follows:

$$V_x = P_1 - \int_{y_m}^{a/2} \int_{-b/2}^{b/2} \sigma(x, y) dx dy = P_1 - \frac{P_1 + P_2}{a} \left(\frac{a}{2} - y_m \right) \quad (20)$$

Now the equation (20) is equal to zero and we obtain:

$$y_m = \frac{a}{2} - \frac{P_1 a}{P_1 + P_2} \quad (21)$$

Then the maximum moment is obtained as follows:

$$M_{c'} = P_1 \left(\frac{a}{2} - \frac{c_1}{2} - y_m \right) - \frac{P_1 + P_2}{2a} \left(\frac{a}{2} - y_m \right)^2 \quad (22)$$

Substituting the equation (21) into equation (22) is:

$$M_{c'} = \frac{P_1 [P_1(a - c_1) - P_2 c_1]}{2(P_1 + P_2)} \quad (23)$$

2.2.1.5. Moment around the axis d'-d'

The resultant force “ $F_{Rd'}$ ” is the force “ P_1 ” acting on column 1 less the volume of pressure the area formed by the axis $d'-d'$ and the corners 1 and 2, which is found to the left of the footing, this is as follows:

$$\begin{aligned} F_{Rd'} &= P_1 - \int_{-L+(a-c_1+c_3)/2}^{a/2} \int_{-b/2}^{b/2} \sigma(x, y) dx dy \\ &= P_1 - \frac{P_1 + P_2}{a} \left(L + \frac{c_1 - c_3}{2} \right) \end{aligned} \quad (24)$$

The moment around the axis $d'-d'$ is:

$$M_{d'} = P_1 \left(L - \frac{c_3}{2} \right) - \frac{P_1 + P_2}{2a} \left(L + \frac{c_1 - c_3}{2} \right)^2 \quad (25)$$

2.2.1.6. Moment around the axis e'-e'

The resultant force “ $F_{Re'}$ ” is the sum of the force “ P_1 ” acting on column 1 and the force “ P_2 ” acting on column 2 less the volume of pressure the area formed by the axis $e'-e'$ and the corners 1 and 2, which is found to the left of the footing, this is as follows:

$$\begin{aligned} F_{Re'} &= P_1 + P_2 - \int_{-L+(a-c_1-c_3)/2}^{a/2} \int_{-b/2}^{b/2} \sigma(x, y) dx dy \\ &= P_1 + P_2 - \frac{P_1 + P_2}{a} \left(L + \frac{c_1 + c_3}{2} \right) \end{aligned} \quad (26)$$

The moment around the axis $e'-e'$ is:

$$M_{e'} = P_1 \left(L + \frac{c_3}{2} \right) + \frac{P_2 c_3}{2} - \frac{P_1 + P_2}{2a} \left(L + \frac{c_1 + c_3}{2} \right)^2 \quad (27)$$

2.2.2. Model to obtain the bending shear

The critical sections for bending shear are obtained at a distance “ d ” starting the junction of the column with the footing as seen in Fig. 7, these are presented in sections $f'_1-f'_1$, $f'_2-f'_2$, $g'-g'$, $h'-h'$ and $i'-i'$.

2.2.2.1. Bending shear in axis $f'_1-f'_1$

Bending shear acting on the axis $f'_1-f'_1$ of the footing “ $V_{ff'_1}$ ” is obtained through the volume of pressure the area formed by the axis $f'_1-f'_1$ with a width “ $b_1 = c_1 + d/2$ ” and the

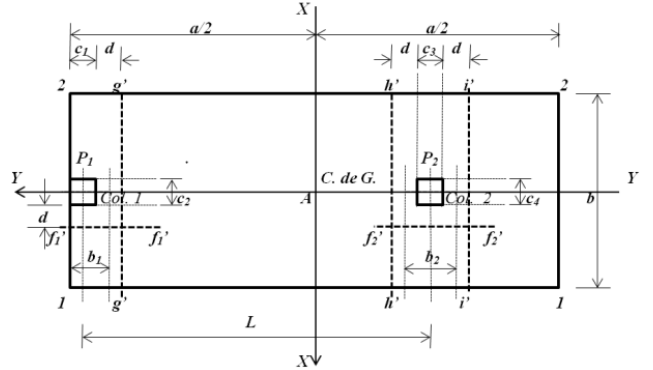


Figure 7. Critical sections for bending shear.

Source: Prepared by the author.

free end of the rectangular footing, where the greatest pressure is presented:

$$\begin{aligned} V_{ff'_1} &= \int_{a/2-b_1}^{a/2} \int_{c_2/2+d}^{b/2} \sigma_{P_1}(x, y) dx dy \\ &= \frac{P_1(b - c_2 - 2d)}{2b} \\ &\quad + \frac{3M_{y1}[b^2 - (c_2 + 2d)^2]}{2b^3} \end{aligned} \quad (28)$$

2.2.2.2. Bending shear in axis $f'_2-f'_2$

Bending shear acting on the axis $f'_2-f'_2$ of the footing “ $V_{ff'_2}$ ” is obtained through the volume of pressure the area formed by the axis $f'_2-f'_2$ with a width “ $b_2 = c_3 + d$ ” and the free end of the rectangular footing, where the greatest pressure is presented:

$$\begin{aligned} V_{ff'_2} &= \int_{(a-c_1-b_2)/2-L}^{(a-c_1+b_2)/2-L} \int_{c_4/2+d}^{b/2} \sigma_{P_2}(x, y) dx dy \\ &= \frac{P_2(b - c_4 - 2d)}{2b} \\ &\quad + \frac{3M_{y2}[b^2 - (c_4 + 2d)^2]}{2b^3} \end{aligned} \quad (29)$$

2.2.2.3. Bending shear in axis $g'-g'$

Bending shear acting on the axis $g'-g'$ of the footing “ $V_{fg'}$ ” is the force “ P_1 ” acting on column 1 less the volume of pressure the area formed by the axis $g'-g'$ and the corners 1 and 2 to the left of the footing, this is as follows:

$$\begin{aligned} V_{fg'} &= P_1 - \int_{a/2-c_1-d}^{a/2} \int_{-b/2}^{b/2} \sigma(x, y) dx dy \\ &= P_1 - \frac{(P_1 + P_2)(c_1 + d)}{a} \end{aligned} \quad (30)$$

2.2.2.4. Bending shear in axis $h'-h'$

Bending shear acting on the axis $h'-h'$ of the footing “ $V_{fh'}$ ” is the force “ P_1 ” acting in column 1 less the volume of pressure the area formed by the axis $h'-h'$ and the corners

1 and 2, which is found to the left of the footing, this is:

$$V_{fh'} = P_1 - \int_{-L+(a-c_1+c_3)/2+d}^{a/2} \int_{-b/2}^{b/2} \sigma(x, y) dx dy \\ = P_1 - \frac{P_1 + P_2}{a} \left(L + \frac{c_1 - c_3}{2} - d \right) \quad (31)$$

2.2.2.5. Bending shear in axis i'-i'

Bending shear acting on the axis $i'-i'$ of the footing “ $V_{fi'}$ ” is the sum of the force “ P_1 ” acting on column 1 and the force “ P_2 ” acting on column 2 less the volume of pressure the area formed by the axis $i'-i'$ and the corners 1 and 2, which is found to the left of the footing, this:

$$V_{fi'} = P_1 + P_2 - \int_{-L+(a-c_1-c_3)/2-d}^{a/2} \int_{-b/2}^{b/2} \sigma(x, y) dx dy \\ = P_1 + P_2 - \frac{P_1 + P_2}{a} \left(L + \frac{c_1 + c_3}{2} + d \right) \quad (32)$$

2.2.3. Model to obtain the punching shear

The critical section for the punching shear appears at a distance “ $d/2$ ” starting the junction of the column with the footing in the two directions.

2.2.3.1. Punching shear for boundary column

The critical section for the punching shear is presented in rectangular section formed by points 3, 4, 5 and 6, as shown in Fig. 8. Punching shear acting on the footing “ V_{p1} ” is the force “ P_1 ” which acting on column 1 less the volume of pressure the area formed by the points 3, 4, 5 and 6:

$$V_{p1} = P_1 - \int_{(a-d)/2-c_1}^{a/2} \int_{-(c_2+d)/2}^{(c_2+d)/2} \sigma(x, y) dx dy \\ = P_1 - \frac{(P_1 + P_2)(c_1 + d/2)(c_2 + d)}{ab} \quad (33)$$

2.2.3.2. Punching shear for inner column

The critical section for the punching shear is presented in rectangular section formed by points 7, 8, 9 and 10, as shown in Fig. 8. Punching shear acting on the footing “ V_{p2} ” is the force “ P_2 ” which acting on column 2 less the volume of pressure the area formed by the points 7, 8, 9 and 10:

$$V_{p2} = P_2 - \int_{(a-d-c_1-c_3/2)-L}^{(a+d-c_1+c_3/2)-L} \int_{-(c_4+d)/2}^{(c_4+d)/2} \sigma(x, y) dx dy \\ = P_2 - \frac{(P_1 + P_2)(c_3 + d)(c_4 + d)}{ab} \quad (34)$$

2.3. Classic model

This model takes into account only the maximum pressure of the soil for design of footings and it is considered uniform at all points on contact area of footings. The maximum pressure is:

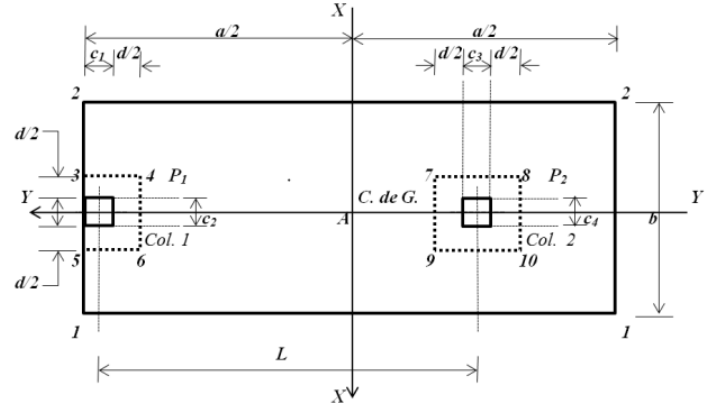


Figure 8. Critical sections for punching shear.
Source: Prepared by the author.

- In the longitudinal direction:

$$\sigma_{max} = \frac{P_1 + P_2}{ab} + \frac{6(M_{y1} + M_{y2})}{ab^2} \quad (35)$$

- In the transverse direction:
 - ❖ To the boundary column is:

$$\sigma_{P_1 max} = \frac{P_1}{b_1 b} + \frac{6M_{y1}}{b_1 b^2} \quad (36)$$

- ❖ To the intermediate column is:

$$\sigma_{P_2 max} = \frac{P_2}{b_2 b} + \frac{6M_{y2}}{b_2 b^3} \quad (37)$$

2.3.1. Model to obtain the moments

Critical sections for bending moments are shown in Fig. 6, these are presented in sections $a_1'-a_1'$, $a_2'-a_2'$, $b'-b'$, $c'-c'$, $d'-d'$ and $e'-e'$. The bending moment in each section is:

$$M_{a_1'} = \frac{\sigma_{P_1 max} b_1 (b - c_2)^2}{8} \quad (38)$$

$$M_{a_2'} = \frac{\sigma_{P_2 max} b_2 (b - c_4)^2}{8} \quad (39)$$

$$M_{b'} = \frac{(P_1 - \sigma_{max} b c_1) c_1}{2} \quad (40)$$

$$M_{c'} = P_1 \left(\frac{a}{2} - \frac{c_1}{2} - \frac{P_1}{\sigma_{max} b} \right) - \frac{\sigma_{max} b}{2} \left(\frac{a}{2} - \frac{P_1}{\sigma_{max} b} \right)^2 \quad (41)$$

$$M_{d'} = P_1 \left(L - \frac{c_3}{2} \right) - \frac{\sigma_{max} b}{2} \left(L + \frac{c_1 - c_3}{2} \right)^2 \quad (42)$$

$$M_{e'} = P_1 \left(L + \frac{c_3}{2} \right) + P_2 \left(\frac{c_3}{2} \right) - \frac{\sigma_{max} b}{2} \left(L + \frac{c_1 + c_3}{2} \right)^2 \quad (43)$$

2.3.2. Model to obtain the bending shear

The critical sections for bending shear (seen in Fig. 7), these are presented in sections $f_1'-f_1'$, $f_2'-f_2'$, $g'-g'$, $h'-h'$ and $i'-i'$. The bending shear in each section is:

$$V_{f_1'} = \frac{\sigma_{P_1 \max} b_1 (b - c_2 - 2d)}{2} \quad (44)$$

$$V_{f_2'} = \frac{\sigma_{P_2 \max} b_2 (b - c_4 - 2d)}{2} \quad (45)$$

$$V_{fg'} = P_1 - \sigma_{\max} b (c_1 + d) \quad (46)$$

$$V_{fh'} = P_1 - \sigma_{\max} b \left(L + \frac{c_1 - c_3}{2} - d \right) \quad (47)$$

$$V_{fi'} = P_1 + P_2 - \sigma_{\max} b \left(L + \frac{c_1 + c_3}{2} + d \right) \quad (48)$$

2.3.3. Model to obtain the punching shear

The critical sections for the punching shear are presented in Fig. 8.

❖ The punching shear for boundary column

$$V_{p1} = P_1 - \sigma_{\max} (c_1 + d/2)(c_2 + d) \quad (49)$$

❖ The punching shear for inner column

$$V_{p2} = P_2 - \sigma_{\max} (c_3 + d)(c_4 + d) \quad (50)$$

2.4. Procedure of design

Step 1: The mechanical elements (P , M_x , M_y) acting on the footing is obtained by the sum of: the dead loads, live loads and accidental loads (wind or earthquake) from each of these effects [20,21].

Step 2: The available load capacity the soil “ σ_{adm} ” is [20, 21]:

$$\sigma_{adm} = q_a - \gamma_{ppz} - \gamma_{pps} \quad (51)$$

where: q_a is the allowable load capacity the soil, γ_{ppz} is the self-weight of the footing, γ_{pps} is the self-weight the soil fill.

Step 3: The value of “ a ” is selected according to the following equation:

$$a = 2 \left(\frac{c_1}{2} + \frac{P_2 L - M_x}{R} \right) \quad (52)$$

where: a is the dimension of the parallel footing the axis “ Y ”, $R=P_1+P_2$, $M_x=M_{x1}+M_{x2}$.

The value of “ b ” is:

To $x_R \leq b/6$:

$$b = \frac{R + \sqrt{R^2 + 24\sigma_{adm} a M_y}}{2\sigma_{adm} a} \quad (53)$$

To $x_R \geq b/6$:

$$b = \frac{2M_y}{R} + \frac{4R}{3\sigma_{adm} a} \quad (54)$$

where: b is the dimension of the parallel footing the axis “ X ”, $M_y=M_{y1}+M_{y2}$.

Note: if in the combinations are included the wind and/or the earthquake, the load capacity the soil should be increased by 33% [18].

Step 4: The mechanical elements (P , M_x , M_y) acting on the footing are factored [18].

Step 5: The bending moments acting on the combined footing are obtained.

Step 6: The effective depth “ d ” for the maximum moment is found by the following expression [18]:

$$d = \sqrt{\frac{M_u}{\emptyset_f b_w \rho f_y \left[1 - \frac{0.59\rho f_y}{f'_c} \right]}} \quad (55)$$

where: M_u is the factored maximum moment at section acting on the footing, \emptyset_f is the strength reduction factor by bending and its value is 0.90, b_w is width of analysis in structural member, ρ is ratio of “ As ” to “ $b_w d$ ”, f_y is the specified yield strength of reinforcement of steel, f'_c is the specified compressive strength of concrete at 28 days.

Step 7: Bending shear resisted by the concrete “ V_{cf} ” is [18]:

$$\emptyset_v V_{cf} = 0.17 \emptyset_v \sqrt{f'_c} b_w d \quad (56)$$

To bending shear acting on the footing (V_f) is compared vs. bending shear resisting by concrete (V_{cf}) and is [18]:

$$V_f \leq \emptyset_v V_{cf} \quad (57)$$

where: \emptyset_v is the strength reduction factor by shear is 0.85.

Step 8: Punching shear (shear force bidirectional) resisted by the concrete “ V_{cp} ” is given [18]:

$$\emptyset_v V_{cp1} = 0.17 \emptyset_v \left(1 + \frac{2}{\beta_c} \right) \sqrt{f'_c} b_0 d \quad (58a)$$

where: β_c is the ratio of long side to short side of the column and b_0 is the perimeter of the critical section.

$$\emptyset_v V_{cp2} = 0.083 \emptyset_v \left(\frac{\alpha_s d}{b_0} + 2 \right) \sqrt{f'_c} b_0 d \quad (58b)$$

where: α_s is 40 for interior columns, 30 for edge columns, and 20 for corner columns.

$$\emptyset_v V_{cp3} = 0.33 \emptyset_v \sqrt{f'_c} b_0 d \quad (58c)$$

where: $\emptyset_v V_{cp}$ must be the value smallest of equations (58a), (58b) and (58c).

To punching shear acting on the footing (V_p) is compared vs. punching shear resisting by concrete (V_{cp}) and must comply with the following expression [18]:

$$V_p \leq \phi_v V_{cp} \quad (59)$$

Step 9: The main reinforcement steel “ A_{sp} ” is [18]:

$$A_{sp} = wb_w d - \sqrt{(wb_w d)^2 - \frac{2M_u w b_w}{\phi_f f_y}} \quad (60)$$

where: w is $0.85f'_c/f_y$.

The minimum steel “ A_{smin} ” and the minimum percentage “ ρ_{min} ” by rule are [18]:

$$A_{smin} = \rho_{min} b_w d \quad (61)$$

$$\rho_{min} = \frac{1.4}{f_y} \quad (62)$$

The reinforcement steel by temperature is found [18]:

$$A_{st} = 0.0018 b_w t \quad (63)$$

where: t is the total thickness of the footing.

Step 10: The development length in tension of deformed bars “ l_d ” is expressed [18]:

Steel reinforcement in the top:

$$l_d = \frac{f_y \psi_t \psi_e}{1.7 \lambda \sqrt{f'_c}} d_b \quad (64)$$

Steel reinforcement in the bottom:

$$l_d = \frac{f_y \psi_t \psi_e}{2.1 \lambda \sqrt{f'_c}} d_b \quad (65)$$

where: ψ_t is the traditional reinforcement location factor to reflect the adverse effects of the top reinforcement casting position, ψ_e is a coating factor reflecting the effects of epoxy coating, d_b is the diameter of the bars, λ is modification factor reflecting the reduced mechanical properties of lightweight concrete, all relative to normalweight concrete of the same compressive strength.

The development length for deformed bars “ l_d ” is compared vs. the available length of the footing “ l_a ” and must comply with the following expression [18]:

$$l_d \leq l_a \quad (66)$$

3. Application

The design of a boundary combined footing supporting two square columns is presented in Fig. 9, with the basic information following: $c_1 = 40 \times 40 \text{ cm}$; $c_2 = 40 \times 40 \text{ cm}$; $L = 6.00 \text{ m}$; $H = 1.5 \text{ m}$; $M_{Dx1} = 140 \text{ kN-m}$; $M_{Lx1} = 100 \text{ kN-m}$; $M_{Dy1} = 120 \text{ kN-m}$; $M_{Ly1} = 80 \text{ kN-m}$; $P_{D1} = 700 \text{ kN}$; $P_{L1} =$

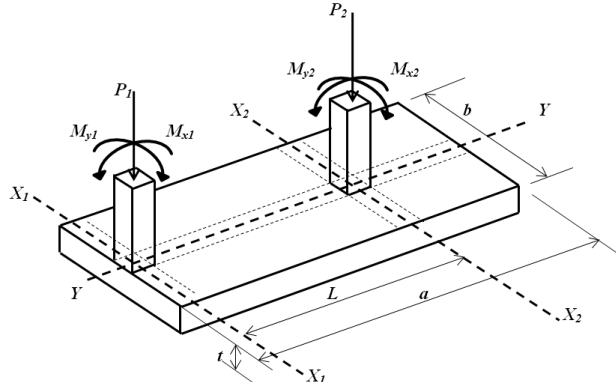


Figure 9. Combined footing supporting two square columns.
Source: Prepared by the author.

500 kN; $M_{Dx2} = 280 \text{ kN-m}$; $M_{Lx2} = 200 \text{ kN-m}$; $M_{Dy2} = 240 \text{ kN-m}$; $M_{Ly2} = 160 \text{ kN-m}$; $P_{D2} = 1400 \text{ kN}$; $P_{L2} = 1000 \text{ kN}$; $f'_c = 21 \text{ MPa}$; $f_y = 420 \text{ MPa}$; $q_a = 220 \text{ kN/m}^2$; $\gamma_{ppz} = 24 \text{ kN/m}^3$; $\gamma_{ppz} = 15 \text{ kN/m}^3$.

Where: H is the depth of the footing, P_D is the dead load, P_L is the live load, M_{Dx} is the moment around the axis “ $X-X$ ” of the dead load, M_{Lx} is the moment around the axis “ $X-X$ ” of the live load, M_{Dy} is the moment around the axis “ $Y-Y$ ” of the dead load, M_{Ly} is the moment around the axis “ $Y-Y$ ” of the live load.

Step 1: The loads and moments acting on soil: $P_1 = 1200 \text{ kN}$; $M_{x1} = 240 \text{ kN-m}$; $M_{y1} = 200 \text{ kN-m}$; $P_2 = 2400 \text{ kN}$; $M_{x2} = 480 \text{ kN-m}$; $M_{y2} = 400 \text{ kN-m}$.

Step 2: The available load capacity the soil: The thickness “ t ” of the footing is proposed, the first proposal is the minimum thickness of 25 cm marking regulations, subsequently the thickness is revised to meet the following conditions: moments, bending shear and punching shear. If such conditions are not satisfied is proposed a greater thickness until it fulfills the three conditions mentioned. The thickness of the footing that fulfills the three conditions listed above is 95 cm for new model and for classic model is 120 cm. Using the equation (51) is obtained the available load capacity of the soil “ σ_{adm} ” is 188.95 kN/m² (new model) and 186.70 kN/m² (classic model).

Step 3: The value of “ a ” by equation (52) is obtained: $a = 8.00 \text{ m}$. The value of “ b ” by equation (53) is found: $b = 3.20 \text{ m}$. These values are for the two models. This value of “ b ” is verified to $x_R \leq b/6$ and meets.

Step 4: The mechanical elements (P , M_x , M_y) acting on the footing is factored: $P_{ul} = 1640 \text{ kN}$; $M_{ux1} = 328 \text{ kN-m}$; $M_{uy1} = 272 \text{ kN-m}$; $P_{u2} = 3280 \text{ kN}$; $M_{ux2} = 656 \text{ kN-m}$; $M_{uy2} = 544 \text{ kN-m}$.

Step 5: The bending moments acting on the footing of the two models are presented in Table 1.

Table 1.
Bending moments

Moments	New model (kN-m)	Classic model (kN-m)
Parallel to axis “Y-Y”		
$M_{a_1'}$	612.88	658.44
$M_{a_2'}$	1225.77	1316.88
Parallel to axis “X-X”		
$M_{b'}$	278.80	263.50
$M_{c'}$	1858.67	1338.33
$M_{d'}$	-1558.00	-5000.32
$M_{e'}$	-1771.20	-6343.80

Source: Prepared by the author.

Table 2.
Dimensions

Concept	New model (cm)	Classic model (cm)
Parallel to axis "Y-Y"	44.35	42.02
Parallel to axis "X-X"	34.41	63.57
Effective depth after performing different proposals	87	112
Coating	8	8
Total thickness	95	120

Source: Prepared by the author.

Table 3.
Bending shear

Bending shear	New model (kN)	Classic model (kN)
Parallel to axis "Y-Y"		
$\phi_v V_{cf_1}$	481.04	711.98
$V_{ff_1'}$	342.10(O.K.)	188.13(O.K.)
$\phi_v V_{cf_2}$	731.65	1127.30
$V_{ff_2'}$	684.21(O.K.)	376.25(O.K.)
Parallel to axis "X-X"		
$\phi_v V_{cf}$	1843.52	2373.26
$V_{fg'}$	858.95(O.K.)	616.08(O.K.)
$V_{fh'}$	-1514.95(O.K.)	-2294.45(O.K.)
$V_{fi'}$	448.95(O.K.)	-1142.92(O.K.)

Source: Prepared by the author.

Table 4.
Punching shear

Punching shear	New model (kN)	Classic model (kN)
Boundary column		
$\phi_v V_{cp1}$	5081.19	7653.77
$\phi_v V_{cp2}$	8995.07	14657.68
$\phi_v V_{cp3}$	3287.83	4952.44
V_{p1}	1436.19(O.K.)	1272.35(O.K.)
Intermediate column		
$\phi_v V_{cp1}$	8779.74	13527.59
$\phi_v V_{cp2}$	12645.97	20625.03
$\phi_v V_{cp3}$	5681.01	8753.14
V_{p2}	2970.02(O.K.)	2697.89(O.K.)

Source: Prepared by the author.

Step 6: The effective depth for the bending moment is found by equation (55); these are shown in Table 2.

Step 7: Bending shear appear in Table 3.

Step 8: Punching shear is presented in Table 4.

Step 9: The reinforcement steel is shown in Table 5.

Step 10: The minimum development length for deformed bars appear in Table 6.

Fig. 10 shows the dimensions and the reinforcement steel of the boundary combined footing for the two models.

4. Conclusions

The foundation is a part essential of a structure, because permits the transmission of loads from the structure to the soil. The mathematical approach suggested in this paper produces results that have a tangible accuracy for all problems, main part of this research for find the solution more economical.

The proposed model presented in this paper for the structural design of boundary combined footings subjected

Table 5.
Reinforcement steel

Reinforcement steel	New model cm ²	Classic model cm ²
Longitudinal reinforcement steel (direction of axis "Y")		
Steel at the top	Main steel	57.94
	Minimum steel	92.71
	Steel proposed	96.27(19Ø1")
Steel in the bottom	Main steel	55.14
	Minimum steel	92.71
	Steel proposed	96.27(19Ø1")
Transverse reinforcement steel (direction of axis "X")		
Steel at the top	Temperature steel	136.80
	Steel proposed	136.81(48Ø3/4")
Steel in the bottom under the boundary column	Main steel	19.24
	Minimum steel	24.19
	Steel proposed	25.65(9Ø3/4")
Steel in the bottom under the inner column	Main steel	38.88
	Minimum steel	36.79
	Steel proposed	39.90(14Ø3/4")
Steel in bottom of the excess parts of the columns	Temperature steel	100.80
	Steel proposed	102.61(36Ø3/4")
		119.71(42Ø3/4")

Source: Prepared by the author.

Table 6.
Development length

Concept	Steel at the top	Steel in the bottom
ψ_t	1.3	1.0
$\psi_e = \lambda$	1.0	1.0
$l_d(\text{cm})$	178.02	83.36
$l_a(\text{cm})$	259.00(O.K.)	132.00(O.K.)

Source: Prepared by the author.

to an axial load and moment in two directions, also it can be applied to others cases: 1) The footings subjected to a concentric axial load, 2) The footings subjected to a axial load and moment in one direction.

The model presented in this paper applies only for design of boundary combined footings, the structural member is assumed to be rigid and the supporting soil layers elastic, which meet expression of the bidirectional bending, i.e., the variation of pressure is linear. The suggestions for future research, when is presented another type of soil, by example in totally cohesive soils (clay soils) and totally granular soils (sandy soils), the pressure diagram is not linear and should be treated differently (see Fig. 1).

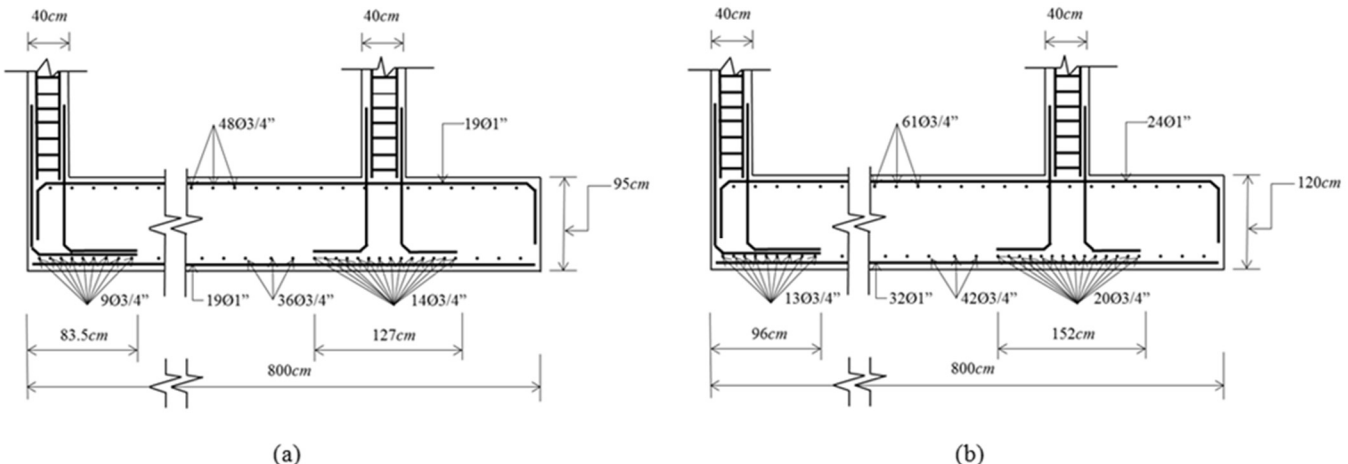


Figure 10. Final design of the boundary combined footing: (a) New model; (b) Classic model.
Source: Prepared by the author.

References

- [1] Bowles, J.E., Foundation analysis and design, McGraw-Hill, New York, 1996.
- [2] Das, B.M., Sordo-Zabay, E. and Arrioja-Juárez, R., Principios de ingeniería de cimentaciones, Cengage Learning Latin America, México, 2006.
- [3] Calabera-Ruiz, J., Calculo de estructuras de cimentación, Intemac Ediciones, México, 2000.
- [4] Tomlinson, M.J., Cimentaciones, diseño y construcción, Trillas, México, 2008.
- [5] Mosley, W.H., Bungey, J.H. and Hulse, R., Reinforced concrete design, Palgrave Macmillan, New York, 1999.
- [6] Gambhir, M.L., Fundamentals of reinforced concrete design, Prentice-Hall, of India Private Limited, 2008.
- [7] Kurian, N.P., Design of foundation systems, Alpha Science Int'l Ltd., India, 2005.
- [8] Pummia, B.C., Kumar-Jain, A., and Kumar-Jain, A., Limit state design of reinforced concrete, Laxmi Publications (P) Limited, New Delhi, India, 2007.
- [9] Varghese, P.C., Design of reinforced concrete foundations, PHI Learning Pvt. Ltd., New Delhi, India, 2009.
- [10] Ibañez-Mora, L., Pruebas de carga no destructivas en pilotes, DYNA, 75 (155), pp. 57-61, 2008.
- [11] Gaviria, C.A., Gómez, D. and Thomson, P., Evaluación de la integridad de cimentaciones profundas: análisis y verificación in situ, DYNA, 76 (159), pp. 23-33, 2009.
- [12] Valencia, Y., Camapum, J. and Lara, L., Aplicaciones adicionales de los resultados de pruebas de carga estáticas en el diseño geotécnico de cimentaciones, DYNA, 175, pp. 182-190, 2012.
- [13] Camacho-Tauta, J.F., Reyes-Ortiz, O.J. and Jimenez-Alvarez, J.D., Comparison between resonant-column and bender element test on three types of soils, DYNA, 80 (182), pp. 163-172, 2013.
- [14] Luévanos-Rojas, A., A mathematical model for dimensioning of footings rectangular, ICIC Express Letters Part B: Applications, 4, pp.269-274, 2013.
- [15] Luévanos-Rojas, A., A mathematical model for dimensioning of footings square, International Review Civil Engineering (IRECE), 3, pp.346-350, 2012.
- [16] Luévanos-Rojas, A., A mathematical model for the dimensioning of circular footings, Far East Journal of Mathematical Sciences, 71, pp. 357-367, 2012.
- [17] Luévanos-Rojas, A., Faudoa-Herrera, J.G., Andrade-Vallejo, R.A. and Cano-Alvarez, M.A., Design of isolated footings of rectangular form using a new model, International Journal of Innovative Computing, Information and Control, 9, pp. 4001-4022, 2013.

- [18] ACI 318S-13 (American Concrete Institute), Building Code Requirements for Structural Concrete and Commentary, Committee 318, 2013.
- [19] Gere, J.M. and Goodo, B.J., Mecánica de materiales, Cengage Learning, México, 2009.
- [20] González-Cuevas, O.M. and Robles-Fernández-Villegas, F., Aspectos fundamentales del concreto reforzado, Limusa, México, 2005.
- [21] McCormac, J.C. and Brown, R.H., Design of reinforced concrete, John Wiley & Sons, New York, 2013.

A. Luévanos-Rojas, received the BSc. Eng in Civil Engineering in 1981, the MSc degree in Planneation and Construction in 1996, and the Engineering Dr. degree in Planneation and Construction in 2009, all of them from the Facultad de Ingeniería, Ciencias y Arquitectura of the Universidad Juárez del Estado de Durango, Gómez Palacio, Durango, México. The MSc degree in Structures in 1983, from the Escuela Superior de Ingeniería y Arquitectura del Instituto Politécnico Nacional, Distrito Federal, México. The MSc degree in Administration in 2004, from the Facultad de Contaduría y Administración of the Universidad Autónoma de Coahuila, Torreón, Coahuila, México. From 1983 to 2009, he is a full time professor and from 2009 to 2014, he is professor and researcher for the Facultad de Ingeniería, Ciencias y Arquitectura of the Universidad Juárez del Estado de Durango. His research interests include: mathematical models applied to structures: methods of structural analysis, members design of concrete and steel, analysis of non-prismatic members. Also he is Associate Editor the journal "ICIC Express Letters Part B: Applications". ORCID: 0000-0002-0198-3614.